

Diverging giant magnetoresistance in ferromagnet-superconductor-ferromagnet trilayers

Soumen Mandal,¹ R. C. Budhani,^{1,*} Jiaqing He,² and Y. Zhu²

¹Condensed Matter-Low Dimensional Systems Laboratory, Department of Physics, Indian Institute of Technology Kanpur, Kanpur-208016, India

²Materials Science Department, Brookhaven National Laboratory, Upton, New York 11973, USA

(Received 1 July 2008; published 4 September 2008)

The relevance of pair-breaking by exchange and dipolar fields, and by injected spins in a low carrier density cuprate $Y_{1-x}Pr_xBa_2Cu_3O_7$ sandwiched between two ferromagnetic $La_{2/3}Sr_{1/3}MnO_3$ layers is examined. At low external field (H_{ext}), the system shows a giant magnetoresistance (GMR), which diverges deep in the superconducting state. We establish a distinct dipolar contribution to magnetoresistance (MR) near the switching field (H_c) of the magnetic layers. At $H_{ext} \gg H_c$, a large positive MR, resulting primarily from the motion of Josephson vortices and pair breaking by the in-plane field, is seen.

DOI: 10.1103/PhysRevB.78.094502

PACS number(s): 74.78.Fk, 72.25.Mk, 74.72.Bk, 75.47.De

I. INTRODUCTION

Electron transport and magnetic ordering in ferromagnet-superconductor (FM-SC) heterostructures display a plethora of novel phenomena,¹⁻⁴ which include pi-phase superconductivity, triplet pairing, field-induced superconductivity, enhanced flux pinning, and related attributes of the two antagonistic orders. These effects acquire increasing richness in systems where the nature of the FM and SC orders is exotic. Thin-film heterostructures of manganites and high-temperature superconducting cuprates offer such systems.⁵⁻¹² The simplest heterostructure which potentially can display some of these phenomena is a trilayer, where a SC film is sandwiched between two ferromagnetic layers. Interestingly, such a structure in the normal state of the SC also constitutes the well-known spin valve in which two ferromagnetic layers sandwich a nonmagnetic (NM) metallic spacer.¹³⁻¹⁶

The giant negative magnetoresistance (MR) seen in FM-NM-FM trilayers and multilayers is related to asymmetric scattering of spin-up and spin-down electrons as they criss-cross the spacer while diffusing along the plane of the heterostructure.¹⁶ This flow of spin-polarized electrons is expected to change profoundly when the spacer material becomes superconducting. Indeed, a large negative magnetoresistance has been seen by Pena *et al.*¹⁰ in $La_{0.7}Ca_{0.3}MnO_3$ - $YBa_2Cu_3O_7$ - $La_{0.7}Ca_{0.3}MnO_3$ (LCMO-YBCO-LCMO) trilayers in the narrow superconducting transition region, which they attribute to spin accumulation in YBCO when the FM layers are coupled antiferromagnetically. The accumulated spins presumably cause depairing and hence a large resistance in accordance with the spin imbalance theory of Takahashi *et al.*¹⁷

In this paper we examine the relevance of pair breaking by the dipolar field and injected spins in a low carrier density cuprate $Y_{1-x}Pr_xBa_2Cu_3O_7$ (YPBCO), which has insulating *c*-axis resistivity and hence a poor spin transmittivity. We further address the issue of giant magnetoresistance (GMR) in three distinctly illuminating ways which involve (i) a current density dependence of MR over a broad range of temperature below T_c , (ii) field dependence of MR when the magnetizations of $La_{2/3}Sr_{1/3}MnO_3$ (LSMO) layers \vec{M}_1 and \vec{M}_2 are parallel and fully saturated, and (iii) dependence of

MR on the angle between current and field below and above the critical temperature. These measurements permit disentanglement of the contributions of flux flow and pair breaking effects in YPBCO, and the intrinsic anisotropic MR of LSMO layers to GMR in FM-SC-FM trilayers, and establish a fundamental theorem which warrants diverging MR in the limit of infinitely conducting spacer.

II. EXPERIMENT

Thin epitaxial trilayers of LSMO-YPBCO-LSMO were deposited on (001) $SrTiO_3$. A multitarget pulsed laser deposition technique based on KrF excimer laser ($\lambda=248$ nm) was used to deposit the single layer films and heterostructure as described in our earlier works.^{9,18} The thickness of each LSMO layer (d_{LSMO}) was left constant at 30 nm whereas the d_{YPBCO} was varied from 30 to 100 nm. The interfacial atomic structure of the trilayers was examined with high-resolution transmission electron microscopy (TEM) at Brookhaven National Laboratory.

The high quality of plane LSMO films and of the films integrated in FM-SC-FM heterostructures has been described in our previous reports.^{9,19} We have also investigated superconductivity in $Y_{1-x}Pr_xBa_2Cu_3O_7$ films as a function of Pr concentration.¹⁸ As for single crystals,²⁰ the T_c of the films^{18,21} also decreases with Pr concentration, and for $x \geq 0.55$, the system has an insulating and antiferromagnetic ground state.²²⁻²⁵ The reduction in T_c with x is presumed to be a consequence of lowering of hole concentration and their mobility due to the out-of-plane disorder caused by Pr ions. Here we concentrate on $x=0.4$ film because of its low carrier density and order parameter phase stiffness,^{18,26} both of which would enhance its susceptibility to pair breaking by spin-polarized carriers injected from the LSMO.

III. RESULTS AND DISCUSSION

Figure 1 shows the resistance $R(T)$ of a trilayer, where the $Y_{0.6}Pr_{0.4}Ba_2Cu_3O_7$ film thickness is ≈ 100 nm and the LSMO layers are 30 nm each. The $R(T)$ curve is characterized by a steep increase in resistivity near ≈ 30 K before the superconductivity sets in at still lower temperatures. While

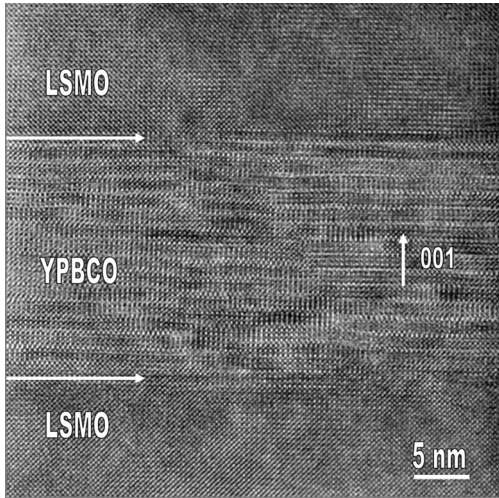
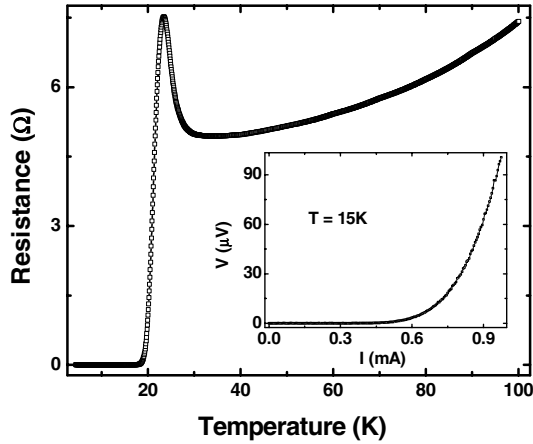


FIG. 1. R vs T curve for a LSMO-YPBCO-LSMO trilayer with 100 nm YPBCO sandwiched between 30 nm each of LSMO layers is shown in the top panel. The rise in resistance at 30 K suggests some structural disorder in the YPBCO film, which presumably localizes the charge carriers before superconductivity sets in at ≈ 24 K. The inset of top panel shows typical I vs V characteristic of the trilayer at 15 K. The bottom panel shows a high-resolution cross-sectional TEM of the trilayer. A careful examination of the lattice image of the superconducting layer shows presence of stacking faults.

$Y_{1-x}Pr_xBa_2Cu_3O_7$ film with $x \geq 0.5$ show superconductor-insulator transition due to carrier localization with a $\rho(T)$ similar to that seen in Fig. 1, for the composition used here ($x=0.4$), the resistivity is expected to remain metallic.^{18,27} The semiconductor-like resistivity seen in Fig. 1 in the temperature window of $T_c < T \leq 30$ K, is likely to be due to structural disorder present in these sandwiched films, some evidence of which comes from high-resolution TEM imaging. The bottom panel of Fig. 1 shows a cross-sectional transmission electron micrograph of the heterostructure. We can clearly see a sharp interface between LSMO and YPBCO in the atomic resolution image. While the manganite layers are free of growth defects, we do see distinct stacking faults in YPBCO, which can be related to the disorder due to difference in ionic radii of Y^{3+} and Pr^{3+} . The inset of Fig. 1 shows a typical current-voltage (I - V) characteristic of the

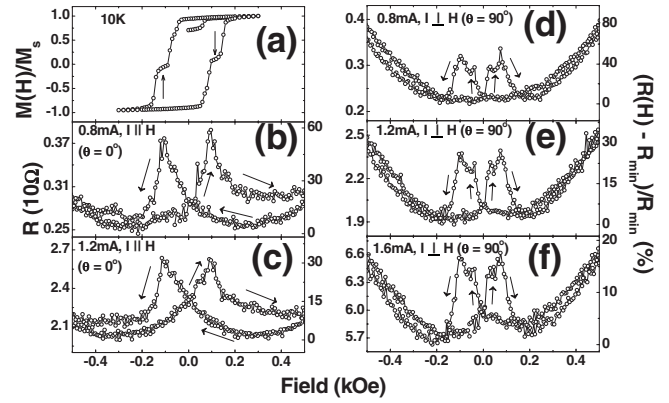


FIG. 2. Panel (a) shows M vs H loop of the trilayer taken at 10 K. The two symmetric small plateaus (indicated by arrows) with zero magnetization show antiferromagnetic coupling between the two FM layers. Panels (b) to (f) show MR measured at 15 K. In panels (b) and (c) the current was parallel to the field, with values 0.8 and 1.2 mA, respectively, whereas for the remaining three panels, the in-plane field was orthogonal to the current ($\theta=90^\circ$), which takes three values: 0.8, 1.2, and 1.6 mA for panels (d), (e), and (f), respectively. The left-hand side of y axis shows resistance in units of 10Ω and the right-hand side of y axis shows $[R(H) - R_{\min}]/R_{\min}$ in percent.

structure at 15 K. The critical current density (J_c) inferred from this measurement is $\sim 5 \times 10^3$ A/cm².

Figure 2 (panel a) shows the magnetic field (\vec{H}) dependence of magnetization (\vec{M}) at 10 K with \vec{H} in the plane of the heterostructure and parallel to the easy axis (110) of LSMO. Starting from a fully saturated magnetic state at $H \approx 180$ Oe, the magnetization reaches a plateau over a field range of -90 to -130 Oe on field reversal. This is indicative of antiferromagnetic (AF) alignment of the magnetization vectors of the top and bottom LSMO films. The full cancellation of the moment ($M \approx 0$) seen in the plateau also suggests that the two layers have equal saturation magnetization (M_s). While a plateau in \vec{M} symmetric about the y axis can also result due to a difference in the switching fields of the top and bottom layers, either because of a difference in their thickness or due to pinning of \vec{M} by the substrate, a perfect cancellation of moments at the plateau indicates antiferromagnetic interlayer exchange mediated by the cuprate spacer. We have demonstrated earlier that the poor c -axis conductivity of YBCO actually quenched the oscillatory part of the interlayer exchange and only an exponentially decaying AF exchange remains in the LSMO-YBCO-LSMO system.⁹ In the remaining five panels of Fig. 2 we show the in-plane resistance of the trilayer as a function of \vec{H} coplanar with the measuring current. Two values of the angle between I and H have been chosen: in one case $\theta=0^\circ$ [Figs. 2(b) and 2(c)] and for the other three panels (d, e, and f) $\theta=90^\circ$ but the magnitude of I is different. While these measurements have been performed at several currents, only a few representative field scans of MR are shown in Fig. 2. The conventional way of measuring MR is to calculate the ratio $\Delta R/R_0$, where $\Delta R=R_H-R_0$, R_0 is the resistance at zero applied field and R_H is the resistance when the applied field

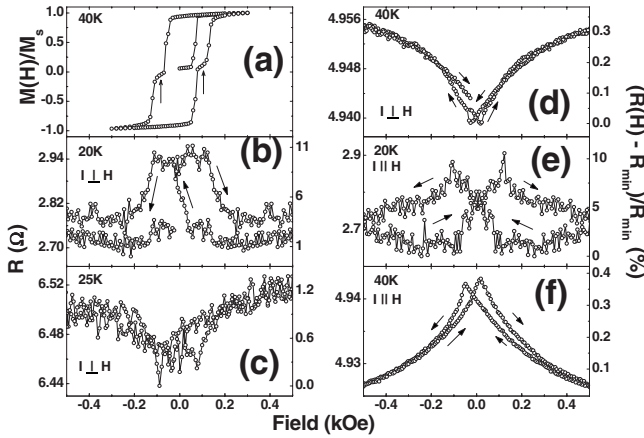


FIG. 3. (a) M vs H loop for the trilayer taken at 40 K. Two symmetric small plateaus (indicated by arrows) with zero magnetization show antiferromagnetic coupling between the two FM layers. Panels (b), (c), and (d) show field dependence of magnetoresistance in $\theta = \pi/2$ ($\vec{I} \perp \vec{H}$) configuration at 20, 25, and 40 K, respectively. Panels (e) and (f) show field dependence of magnetoresistance in $\theta = 0$ ($\vec{I} \parallel \vec{H}$) configuration at 20 and 40 K, respectively. The left-hand side of y axis shows resistance (Ω) and the right-hand side of y axis shows the $[R(H) - R_{\min}]/R_{\min}$ in percent.

is H . Here we have used a slightly different definition. We have replaced R_0 by R_{\min} , which is the minimum resistance seen in R vs H curves. The magnetoresistance for both $\theta = 90^\circ$ and $\theta = 0^\circ$ configurations has two distinct regimes of behavior. Starting from a fully magnetized state at 500 Oe in the $\theta = 90^\circ$ configuration, the MR first drops to a minimum as the field is brought to zero following a dependence of the type $\sim \alpha H + \beta H^2$, where $\alpha = -6.8 \times 10^{-6}$ and $\beta = 7.7 \times 10^{-8}$ for $I = 0.8$ mA. The MR shows a steplike jump at the reversed field of ~ 40 Oe, where the magnetization switched to AF configuration and remains high until \vec{M}_1 and \vec{M}_2 become parallel again. On reversing the field toward positive cycle, a mirror image of the curve is seen in the positive field quadrant. A remarkable feature of the MR seen in Fig. 2 is its dependence on current I . The peak MR at 500 Oe and $I \perp H$ drops from $\sim 80\%$ to 17% on increasing the current by a factor of 2. The height of the MR curves remains nearly the same when the magnetic field is rotated from $\theta = 90^\circ$ to $\theta = 0^\circ$ with some differences in the detailed shape of the curves. The pertinent factors which affect the MR of such structures are (i) the behavior of MR in the normal state of YPBCO, (ii) the explicit role of superconductivity, which is suppressed by the dipolar and exchange fields of the FM layers, and by the spin polarized electrons injected from the FM layers, and (iii) a parasitic nonzero tilt of the sample away from parallel configuration, which will result in a high concentration of vortices in the superconducting spacer even at very low fields. These factors are addressed with the help of Fig. 3, where we have plotted the $M(H)$ loop at 40 K (normal state). The overall shape of this curve is not different from what is seen in the SC state (Fig. 2) except for a temperature-dependent change in the switching fields and M_s . The AF alignment of \vec{M}_1 and \vec{M}_2 in the vicinity of zero field persists in the normal state as well. Figure 3 also shows

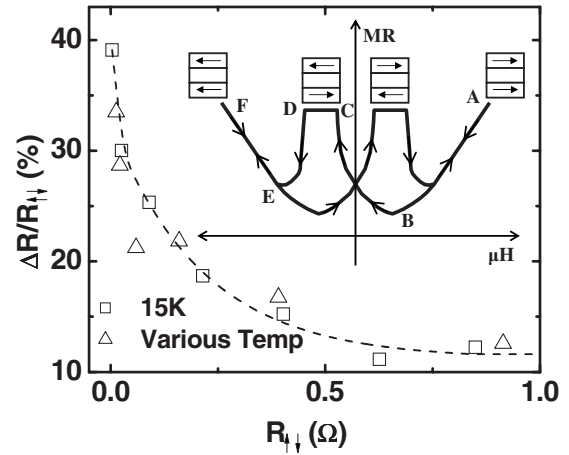


FIG. 4. Dependence of MR on R_{\perp} . This figure contains MR data collected at 15 K with variable current and at several temperatures across the transition at constant current. A remarkable universality of the dependence of MR emerges on the ground-state resistance of the structure. The inset shows a typical sketch of MR vs H curve in the superconducting state and identify some critical points, where \vec{M}_1 & \vec{M}_2 change their orientation (more details in text).

the field dependence of magnetoresistance in $\theta = 90^\circ$ and $\theta = 0^\circ$ configuration at a few representative temperatures as the sample is taken from superconducting to normal state. A striking drop in MR on approaching the normal state is evident in addition to a noticeable change in its field dependence. At 40 K and $\theta = 90^\circ$, it drops monotonically on reducing the field from full saturation until the reverse-switching field is reached, where it shows a small but discernible step-like increase followed by an unremarkable field dependence in the negative field side. For $I \parallel H$ configuration [Fig. 3(f)] the $R(H)$ curve is an inverted image of Fig. 3(d) reflecting the anisotropic magnetoresistance (AMR) of LSMO films. The 20 K data is shown in Figs. 3(b) and 3(e); the MR value is similar with the exception that the antiferromagnetic regime is clearly seen for $I \perp H$.

It becomes clear from Figs. 2 and 3 that the field-dependence of MR in these FM-SC-FM trilayers can be divided into two field regimes, one covering the range $-150 \text{ Oe} < H < 150 \text{ Oe}$, where the reorientation of \vec{M}_1 and \vec{M}_2 is the deciding factor, and at the higher fields where $\vec{M}_1 \parallel \vec{M}_2$ and it goes as $\sim \alpha H + \beta H^2$. While the MR in these regimes is intimately linked with superconductivity of YPBCO, its mechanism appears to be remarkably different. We first concentrate on the low-field regime where we define MR as $(R_{\perp} - R_{\min})/R_{\perp}$, where R_{\perp} and R_{\min} , respectively, are the resistances of the trilayer when \vec{M}_1 and \vec{M}_2 are antiparallel, the plateau region, and R_{\min} is the minimum resistance as defined earlier. The variation of MR with R_{\perp} at a fixed temperature (15 K) with variable current and at several temperatures across the transition at constant current is shown in Fig. 4. A remarkable universality of the dependence of MR emerges on the ground-state resistance of the structure. The magnetoresistance starts with a negligibly small value at $T > T_c$ but then diverges on entering the superconducting state. While an enhancement in MR has been seen in spin valves of

cleaner spacers,^{13,14,16} the regime of diverging MR is only accessible with a superconducting spacer. Unlike the case of free-electron-like metal spacers, where the strength of MR is attenuated by spin-flip scattering processes in the interior of the spacer and at spacer-ferromagnet interfaces,^{16,28} the physics of transport of spin-polarized carriers in FM-SC-FM structures is much more challenging. Here we identify various factors which can contribute to MR and then single out the ones which perhaps are truly responsible for the behavior seen in Fig. 4. In the inset of Fig. 4 we sketch a typical MR vs H curve at $T < T_c$ and identify some critical points on the curve where the orientation of \vec{M}_1 and \vec{M}_2 and the effective magnetic field seen by the SC layer change significantly. We first consider the behavior of MR in a field regime very close to the origin in Fig. 4 (inset). For the AF configuration of \vec{M}_1 and \vec{M}_2 (point C) the dipolar field in the spacer cancels out but for the parallel alignment (point B) it adds up. Thus, strictly from the angle of pair breaking by the dipolar field, the SC layer should have a lower resistance in the AF configuration. Moreover, a much stronger effect of the exchange field of ferromagnetic layers on superconductivity when \vec{M}_1 and \vec{M}_2 are parallel should make the AF state less resistive.¹ Both these effects are inconsistent with the observation of a higher resistance in the AF state. However, before we rule out effects of the dipolar field altogether in influencing MR, a careful examination of the MR curve along the path A \rightarrow B \rightarrow C \rightarrow D \rightarrow E \rightarrow F of the inset traced on reducing the field from parallel alignment of \vec{M}_1 and \vec{M}_2 needs to be made. At point B the dipolar field of ferromagnetically aligned \vec{M}_1 and \vec{M}_2 in the superconductor completely cancels out the positive external field, leading to a minimum in resistance. As the field is reduced to zero and then made negative (between points B and C) the net field seen by the superconductor increases. At the negative coercive field H_c , just before \vec{M}_1 and \vec{M}_2 become antiparallel (point C), the internal field in SC is $B_{\uparrow\downarrow} = -\mu_o H_{\text{ext}} - \mu_o(m_1^d + m_2^d)$, where m_1^d and m_2^d are the dipolar contribution to magnetization in the superconductor. However, just beyond $|H| > H_c$ in the AF state, the internal field ($B_{\uparrow\downarrow}$) is only $\mu_o H_{\text{ext}}$ (assuming $m_1^d \sim m_2^d$). While this sudden reduction in B_{int} at H_c could be responsible for the plateau (segment C-D) seen in $R(H)$ in the AF state, the higher resistance in the AF state still remains a puzzle. Although one could attribute it to piling up of spin-polarized quasiparticles in the SC spacer, such interpretation would require a deeper understanding of c -axis transport in these structures, where the CuO_2 planes are parallel to the magnetic layers. The observation of this effect in a low carrier density cuprate of the present study is much more intriguing because its c -axis resistivity is insulator-like in the normal state.²² The precipitous drop in resistance from point D to E also points toward the critical role of the net internal field in the SC layer and its influence on MR because at point D, the \vec{M}_1 and \vec{M}_2 vectors switch to parallel configuration, leading to an additive dipolar field in the superconductor pointing 180° away from the direction of the external field.

We now discuss the large positive magnetoresistance in the ferromagnetic configuration of \vec{M}_1 and \vec{M}_2 . The field de-

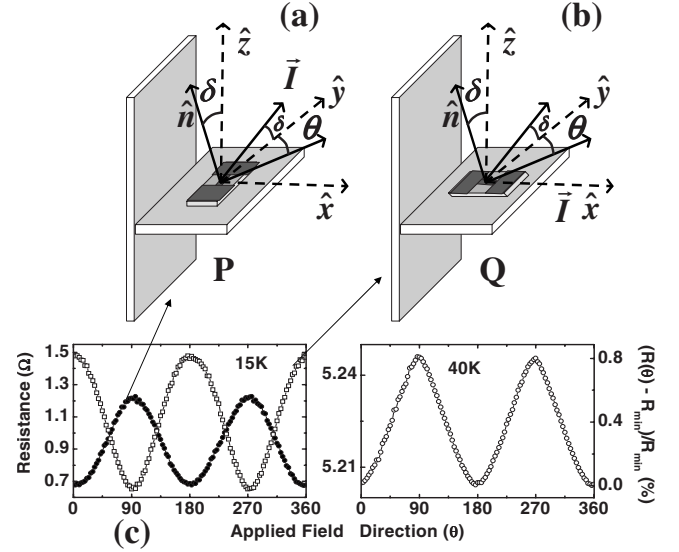


FIG. 5. Panels (a) and (b), respectively, show the configuration P and Q of sample mounting in the cryostat. The sample stage has a nonzero tilt (δ) with respect to the x - y plane. (c) AMR of the trilayer measured at 15 K in configuration P and Q, and at 40 K in configuration P.

pendence of MR in this regime derives contributions from pair breaking effects of spin-polarized electrons injected from LSMO and of the net field seen by the YPBCO. Moreover, a parasitic normal component of the field due to misalignment will introduce vortices and a large dissipation due to flux flow. Here a small negative contribution to R is also expected due to the intrinsic MR of LSMO, which would vary as M^2 . We have estimated the contribution of sample tilt by measuring its resistance in two configurations P and Q as shown in Figs. 5(a) and 5(b). We assume that the platform on which the film is mounted for measurement, instead of being on the x - y plane, has a small tilt δ away from the y axis. In configuration P, the sample is mounted in such a manner that the stripe of film, along which the current flows, is nominally along \hat{y} . Figure 5(b) shows the 90° geometry such that the stripe is now along \hat{x} . This is labeled as configuration Q. We rotate \vec{H} in the x - y plane and measure R as a function of the angle θ between \hat{y} and the field direction. We expect three distinct contributions to $R(\theta)$ coming from (i) vortex dissipation due to normal component of the field [$(\Delta R)_{v\perp}$], (ii) Lorentz force on Josephson vortices in the plane of the film $(\Delta R)_{v\parallel}$, and (iii) the anisotropic magnetoresistance of LSMO layers $(\Delta R)_{\text{AMR}}$, which peaks when I is perpendicular to the in-plane field.^{29,30} While all these contributions to R are periodic in θ with a periodicity of π , in configuration P, $(\Delta R)_{v\perp}$ will peak at $\theta=0$ and π , whereas the peak in $(\Delta R)_{v\parallel}$ and $(\Delta R)_{\text{AMR}}$ will appear at $\theta=\pi/2$ and $3\pi/2$. Since the resistivity of the sample in configuration P peaks at $\pi/2$ and $3\pi/2$ [see Fig. 5(c)], it is evident that $(\Delta R)_{v\perp} < [(\Delta R)_{v\parallel} + (\Delta R)_{\text{AMR}}]$. For configuration Q, on the other hand, $(\Delta R)_{v\perp}$, $(\Delta R)_{v\parallel}$, and $(\Delta R)_{\text{AMR}}$ are all in phase with peak value appearing at $\theta=0$ and π as seen in Fig. 5(c). Clearly, the difference of the peak height at $\theta=0$ of Q and $\theta=\pi/2$ of P gives us the flux flow resistance due to motion of vortices, which nucleate because of a nonzero tilt. Its contribution to resistance is

~10% at 15 K and 3 kOe nominally parallel field. Of course its strength will also vary with current. It is clear that a much larger contribution to +ve MR comes from the in-plane field and its attendant effects.

IV. CONCLUSION

In summary, we have seen an exceedingly large magnetoresistance in $\text{La}_{2/3}\text{Sr}_{1/3}\text{MnO}_3\text{-Y}_{0.6}\text{Pr}_{0.4}\text{Ba}_2\text{Cu}_3\text{O}_7\text{-La}_{2/3}\text{Sr}_{1/3}\text{MnO}_3$ trilayer in the superconducting transition region of the cuprate. The significant feature of these results is the divergence of MR as the resistance of the spacer goes to zero. We identify the key contributing factors to MR in superconductor based spin valves. These are (i) dipolar and

exchange fields in the SC layer, (ii) depairing by accumulation of spin-polarized electrons in the superconductor in the antiferromagnetic state of the spin valve, and (iii) the contribution of vortex motion to resistance. We establish that the dipolar field of the LSMO layer in the superconductor plays a crucial role in setting the scale of MR in the field regime where the magnetization vectors of the FM layers switch from antiparallel to parallel configuration.

ACKNOWLEDGMENTS

This research has been supported by grants from the Board of Research in Nuclear Sciences and the Department of Information Technology, Government of India.

*rcb@iitk.ac.in

- ¹P. G. de Gennes, Phys. Lett. **23**, 10 (1966); G. Deutscher and F. Meunier, Phys. Rev. Lett. **22**, 395 (1969); J. J. Hauser, *ibid.* **23**, 374 (1969).
- ²F. S. Bergeret, A. F. Volkov, and K. B. Efetov, Rev. Mod. Phys. **77**, 1321 (2005); I. F. Lyuksyutov and V. L. Pokrovski, Adv. Phys. **54**, 67 (2005); A. I. Buzdin, Rev. Mod. Phys. **77**, 935 (2005).
- ³J. Y. Gu, C.-Y. You, J. S. Jiang, J. Pearson, Ya. B. Bazaliy, and S. D. Bader, Phys. Rev. Lett. **89**, 267001 (2002); R. S. Keizer, S. T. B. Goennenwein, T. M. Klapwijk, G. Miao, G. Xiao, and A. Gupta, Nature (London) **439**, 825 (2006); John Q. Xiao and C. L. Chien, Phys. Rev. Lett. **76**, 1727 (1996); E. A. Demler, G. B. Arnold, and M. R. Beasley, Phys. Rev. B **55**, 15174 (1997).
- ⁴V. Peña, T. Gredig, J. Santamaria, and I. K. Schuller, Phys. Rev. Lett. **97**, 177005 (2006); Zhaorong Yang, Martin Lange, Alexander Volodin, Ritta Szymczak, and Victor V. Moshchalkov, Nat. Mater. **3**, 793 (2004); David J. Morgan and J. B. Ketterson, Phys. Rev. Lett. **80**, 3614 (1998).
- ⁵N.-C. Yeh, R. P. Vasquez, C. C. Fu, A. V. Samoilov, Y. Li, and K. Vakili, Phys. Rev. B **60**, 10522 (1999).
- ⁶Z. Y. Chen, Amlan Biswas, Igor Žutić, T. Wu, S. B. Ogale, R. L. Greene, and T. Venkatesan, Phys. Rev. B **63**, 212508 (2001).
- ⁷C. A. R. Sá de Melo, Physica C **387**, 17 (2003).
- ⁸Todd Holden, H.-U. Habermeier, G. Cristiani, A. Golnik, A. Boris, A. Pimenov, J. Humlíček, O. I. Lebedev, G. Van Tendeloo, B. Keimer, and C. Bernhard, Phys. Rev. B **69**, 064505 (2004).
- ⁹K. Senapati and R. C. Budhani, Phys. Rev. B **71**, 224507 (2005); **70**, 174506 (2004).
- ¹⁰V. Peña, Z. Sefrioui, D. Arias, C. Leon, J. Santamaria, J. L. Martinez, S. G. E. te Velthuis, and A. Hoffmann, Phys. Rev. Lett. **94**, 057002 (2005); C. Visani, V. Peña, J. Garcia-Barriocanal, D. Arias, Z. Sefrioui, C. Leon, J. Santamaria, N. M. Nemes, M. Garcia-Hernandez, J. L. Martinez, S. G. E. te Velthuis, and A. Hoffmann, Phys. Rev. B **75**, 054501 (2007).
- ¹¹J. Albrecht, S. Soltan, and H.-U. Habermeier, Phys. Rev. B **72**, 092502 (2005).
- ¹²J. Chakhalian, J. W. Freeland, G. Srajer, J. Strempler, G. Khaliullin, J. C. Cezar, T. Charlton, R. Dalgliesh, C. Bernhard, G. Cristiani, H.-U. Habermeier, and B. Keimer, Nat. Phys. **2**, 244 (2006).
- ¹³G. Binasch, P. Grünberg, F. Saurenbach, and W. Zinn, Phys. Rev. B **39**, 4828 (1989).
- ¹⁴M. N. Baibich, J. M. Broto, A. Fert, F. Nguyen Van Dau, F. Petroff, P. Eitenne, G. Creuzet, A. Friederich, and J. Chazelas, Phys. Rev. Lett. **61**, 2472 (1988).
- ¹⁵B. Dieny, V. S. Speriosu, S. Metin, S. S. P. Parkin, B. A. Gurney, P. Baumgart, and D. R. Wilhoit, J. Appl. Phys. **69**, 4774 (1991).
- ¹⁶K. B. Hathaway, in *Ultrathin Magnetic Structures II*, edited by B. Heinrich and J. A. C. Bland (Springer-Verlag, Germany, 1994), pp. 45–194.
- ¹⁷S. Takahashi, H. Imamura, and S. Maekawa, Phys. Rev. Lett. **82**, 3911 (1999); J. Appl. Phys. **87**, 5227 (2000).
- ¹⁸Pengcheng Li, Soumen Mandal, R. C. Budhani, and R. L. Greene, Phys. Rev. B **75**, 184509 (2007).
- ¹⁹M. Golosovsky, M. Abu-Teir, D. Davidov, O. Arnache, P. Monod, N. Bontemps, and R. C. Budhani, J. Appl. Phys. **98**, 084902 (2005).
- ²⁰V. Sandu, E. Cimpoiasu, T. Katuwal, C. C. Almasan, S. Li, and M. B. Maple, Phys. Rev. Lett. **93**, 177005 (2004).
- ²¹Peng Xiong, Gang Xiao, and X. D. Wu, Phys. Rev. B **47**, 5516 (1993).
- ²²R. F. Tournier, D. Isfort, D. Bourgault, X. Chaud, D. Buzon, E. Floch, L. Porcar, and P. Tixado, Physica C **386**, 467 (2003).
- ²³Ratan Lal, Ajay, R. L. Hota, and S. K. Joshi, Phys. Rev. B **57**, 6126 (1998).
- ²⁴I. Felner, U. Yaron, I. Nowik, E. R. Bauminger, Y. Wolfus, E. R. Yacoby, G. Hilscher, and N. Pillmayr, Phys. Rev. B **40**, 6739 (1989).
- ²⁵D. W. Cooke, R. S. Kwok, R. L. Lichti, T. R. Adams, C. Boekema, W. K. Dawson, A. Kebede, J. Schwegler, J. E. Crow, and T. Mihalisin, Phys. Rev. B **41**, 4801 (1990).
- ²⁶J. L. Peng, P. Klavins, R. N. Shelton, H. B. Radousky, P. A. Hahn, and L. Bernardez, Phys. Rev. B **40**, 4517 (1989).
- ²⁷M. Covington and L. H. Greene, Phys. Rev. B **62**, 12440 (2000).
- ²⁸Peter M. Levy, Shufeng Zhang, and Albert Fert, Phys. Rev. Lett. **65**, 1643 (1990).
- ²⁹Soumen Mandal and R. C. Budhani, arXiv:0802.4092, J. Magn. Magn. Mater. (to be published).
- ³⁰L. M. Berndt, Vincent Balbarin, and Y. Suzuki, Appl. Phys. Lett. **77**, 2903 (2000).